Discovery of a Radio Source following the 27 December 2004 Giant Flare from SGR 1806−20

P. B. Cameron[1], P. Chandra[2,3], A. Ray[2], S. R. Kulkarni[1], D. A. Frail[4], M. H. Wieringa[5], E. Nakar[6], E. S. Phinney[6], Atsushi Miyazaki[7], Masato Tsuboi[8], Sachiko Okumura[8], N. Kawai[9], K. M. Menten[10] & F. Bertoldi[11]

[1] Division of Physics, Mathematics and Astronomy, 105-24, California Institute of Technology, Pasadena, CA 91125, USA
[2] Tata Institute of Fundamental Research, Mumbai 400 005, India
[3] Joint Astronomy Programme, Indian Institute of Science, Bangalore 560 012, India
[4] National Radio Astronomy Observatory, Socorro, NM 87801, USA
[5] Australia Telescope National Facility, CSIRO, P.O. Box 76, Epping NSW 1710, Australia
[6] Theoretical Astrophysics 130-33, California Institute of Technology, Pasadena, CA 91125, USA
[7] Shanghai Astronomical Observatory 80 Nandan Road Shanghai 200030, China
[8] Nobeyama Radio Observatory,National Astronomical Observatory of Japan Minamisaku, Nagano 384-1305, Japan
[9] Department of Physics Tokyo Institute of Technology Ookayama 2-12-1, Meguro-ku,Tokyo 152-8551, Japan
[10] Max Planck Institut für Radioastronomie, Auf dem Hügel 69; 53121 Bonn, Germany
[11] University of Bonn, Auf dem Hüegel 71, 53121 Bonn, Germany

Over a decade ago it was established that the remarkable high energy transients, known as soft gamma-ray repeaters (SGRs), are a Galactic population[1,2] and originate from neutron stars with intense ($\lesssim 10^{15}$ G) magnetic fields ("magnetars"[3]). On 27 December 2004 a giant flare[4] (fluence[5] $\gtrsim 0.3$ erg cm^{-2}) was detected from SGR 1806−20. Here we report the discovery of a fading radio counterpart. We began a monitoring program from 0.2 GHz to 250 GHz and obtained a high resolution 21-cm radio spectrum which traces the intervening interstellar neutral Hydrogen clouds. Analysis of the spectrum yields the first direct distance measurement of SGR 1806−20. The source is located at a distance greater than 6.4 kpc and we argue that it is nearer than 9.8 kpc. If true, our distance estimate lowers the total energy of the explosion and relaxes the demands on theoretical models. The energetics and the rapid decay of the radio source are not compatible with the afterglow model that is usually invoked for gamma-ray bursts. Instead we suggest that the rapidly decaying radio emission arises from the debris ejected during the explosion.

On 3 January 2005 we observed SGR 1806−20 with the Very Large Array (VLA) and identified and promptly reported[6] a new radio source at right ascension

$\alpha_{J2000} = 18^{\mathrm{h}}08^{\mathrm{m}}39.34^{\mathrm{s}}$ and declination $\delta_{J2000} = -20°24'39.7''$ (with an uncertainty of ± 0.1" in each coordinate) coincident with the quiescent X-ray counterpart.[7] In Table 1 we report the results of a subsequent monitoring program undertaken with the VLA, the Giant Metrewave Radio Telescope (GMRT), the Australia Telescope Compact Array (ATCA), the Nobeyama Millimeter Array (NMA) and the Institut de Radioastronomie Millimétrique (IRAM) 30m Telescope.

The radio source decays in all frequency bands, but the behaviour is complex (Figure 1). At each band we model the flux by a power law, $S_\nu(t) \propto t^\alpha$, but allow for changes in the temporal indices α ("breaks") at two epochs. These breaks are clearly seen in our highest signal-to-noise ratio data. Following the first break (9 days, postburst) the light curve steepens to $-4 \lesssim \alpha \lesssim -3$. The radio source[8] from SGR 1900+14 following the 27 August 1998 giant flare[9] showed a similar rapid decay at $8\,\mathrm{GHz}$. Subsequently around day 14 the light curve flattens to $\alpha \sim -1$. At any given epoch, the radio spectrum can be modeled by a power law, $S_\nu \propto \nu^\beta$. The spectral index, β, steepens with time, changing from ~ -0.7 to -0.9 (see Figure 1 and Supplemental Information).

We confirm claims that the source is resolved[10] by an independent analysis. We find that it is elongated with a major axis $\theta \sim 77\,$milliarcsecond (mas) and an axial ratio of 2:1 (Table 2). We considered four expansion models, $\theta \propto t^s$ with unconstrained s and plausible expansion models ($s = 0$, 2/5, and 1). The best fit model corresponds to no expansion ($s = 0.04 \pm 0.15$). However, due to the limited range of our observations we prefer not to model the dynamics of the explosion.

We took advantage of the brightness of the radio source and obtained a high resolution spectrum (Figure 2, second panel) centered around the 21-cm line of atomic Hydrogen (HI). Intervening interstellar clouds appear as absorption features in the spectrum. These clouds are expected to participate in the rotation of the Galaxy and the absorption features allow us to infer "kinematic" distance estimates. Such estimates have several complications. First, in the inner Galaxy the radial velocity curve is double-valued (see Figure 2, third panel) leading to a "near" distance estimate (d_l) and a "far" distance estimate (d_u) for each velocity. Second, in some directions, there are features with non-circular motion e.g. the "3-kpc expanding arm" and the "$-30\,\mathrm{km\,s^{-1}}$ spiral arm".[11] Finally, in the innermost part of the Galaxy there is a deficit of cold gas.[12]

Significant HI absorption toward SGR 1806−20 is seen over the velocity range −20 km s^{-1} to +85 km s^{-1} (Figure 2, second panel). There is also a weak (2.5-σ) absorption feature coincident in velocity with a clearly detected ^{12}CO(1-0) emission feature identified[13] as MC94 (Figure 2, first panel). Adopting a simple Galactic rotation curve with a circular velocity $\Theta_{\circ} = 220$ km s^{-1} and a Galactic center distance R$_{\circ}$=8.5 kpc, the near distance to SGR 1806−20 (for V$_{LSR}$=95 km s^{-1}) is d$_l$=6.4 kpc.

The two HI emission clouds seen at velocities above 100 km s^{-1} toward SGR 1806−20 (Figure 2, first panel), with no corresponding HI absorption, may be used to infer an upper limit to the distance provided that we can be reasonably certain that cold neutral gas exists at these velocities. The HI absorption spectrum toward the nearby ($\Delta\theta = 0.77°$) extragalactic source J1811−2055 shows a strong and broad absorption feature between 110 and 130 km s^{-1} (Figure 2, fourth panel). The only HI emission in this direction[14] above 60 km s^{-1} corresponds to an HI cloud at this same velocity. This feature can be traced in absorption toward several other extragalactic radio sources in this direction,[15] suggesting that cold gas at ∼120 km s^{-1} is widespread. Adopting the same Galactic rotation curve as above, the absorbing cloud at +120 km s^{-1} can either be located at 7 kpc or 9.8 kpc (see Figure 2, third panel). We thus suggest an upper limit to the distance, d$_u$=9.8 kpc.

Our new distance estimate is smaller than previous (indirect) values[16,11] of 12 to 15 kpc. Accepting our estimate has several important implications. It results in a reduction of the total energy released ($\propto d^2$) as well as the rate of such events in nearby galaxies[17] ($\propto d^3$), and calls into question the association[18] of SGR 1806−20 with a star cluster along the same line-of-sight. Therefore, claims that magnetars originate from more massive stars than normal neutron stars[19] may be called into question.

Next we consider the energetics of the material giving rise to the radio emission. As with many other radio sources, the power law spectrum can be attributed to energetic electrons with a power law energy distribution ($dN/d\gamma \propto \gamma^{-p}$; here γ is the Lorentz factor of electrons and we measure $p = 2.24 \pm 0.04$ on day 7, which as is a typical value for strong shocks) which gyrate in a magnetic field and emit synchrotron radiation. We apply the minimum energy formulation for synchrotron sources[20,21] to the radio spectrum (from 0.2 GHz to 100 GHz) of 3 January 2005 and find the energy of the radio emitting source and the associated magnetic field strength are $U_{min} \sim 10^{43} d_{10}^{17/7} \theta_{75}^{9/7}$ erg and $B_{min} \sim$

$13d_{10}^{-2/7}\theta_{75}^{-6/7}$ mG; here, the distance is $10d_{10}$ kpc and the angular diameter is $75\theta_{75}$ mas (Table 2).

Evidently the amount of energy released in the γ-ray flare, $E_{\gamma,\text{iso}} \gtrsim 4 \times 10^{45}\,\text{erg}\,\text{s}^{-1}$ (assuming unbeamed, isotropic emission), substantially exceeds U_{min}. In contrast, the ratio $U_{\text{min}}/E_{\gamma,\text{iso}}$ is unity for GRBs and as a result the lower energy and longer duration emission is correctly regarded as arising from the shock of the circumburst medium (the "afterglow" model). Thus, based solely on energetics, there is no *prima facie* reason to suggest that the radio source is the afterglow of the γ-ray flare.

Furthermore, as discussed above, the radio emission decays quite rapidly 9 days after the burst. Such a rapid decay is incompatible with the afterglow model (in the non-relativistic limit) for which we expect[22] $\alpha = 3\beta + 0.6$. We conclude (in contrast to refs. 23, 24 and 25) that the radio emission must be powered by something very different from that which produced the γ-ray emission.

In summary, the radio emission can be described by two components: a rapidly decaying component and a slowly decaying component. The latter becomes detectable when the former has decayed significantly. The rapid decay is phenomenologically similar to that seen from accreting Galactic sources (e.g. ref. 26) – the so-called "plasmon" model framework in which the radio emission arises from a ball of electrons and magnetic field which are initially shocked and then cool down by expansion. We make the specific suggestion that the radio emission up until about 2 weeks is a result of the shocking of the debris given off in the explosion (the "reverse shock"). In this framework the slowly decaying component is the emission arising from the forward shock as the ejecta slams into the circumburst medium. A requirement of this suggestion is that the energy inferred in the slowly decaying component should be comparable to U_{min}. Separately, we note that the comparable ratios $U_{min}/E_{\gamma,\text{iso}}$ and the temporal and spectral similarities of the giant flares from SGR 1806−20 and SGR 1900+14 suggest a common mechanism for launching these flares and similar circumstellar environments.

Regardless of the suggestions and speculations, it is clear that radio afterglow is telling us something entirely different from that revealed by the γ-ray emission. If our suggestion of a reverse shock origin is correct then radio observations allow us to probe the ejecta.

Taken together it appears that rapid and intense radio monitoring of such flares will be highly fruitful in the future.

---

1. Kulkarni, S. R. & Frail, D. A. Identification of a supernova remnant coincident with the soft gamma-ray repeater SGR1806-20. *Nature* **365**, 33–35 (1993).

2. Murakami, T., Tanaka, Y., Kulkarni, S. R., Ogasaka, Y., Sonobe, T. *et al.* X-Ray Identification of the Soft Gamma-Ray Repeater 1806-20. *Nature* **368**, 127–128 (1994).

3. Woods, P. M. & Thompson, C. Soft gamma repeaters and anomalous x-ray pulsars: Magnetar candidates. To appear in 'Compact Stellar X-ray Sources', eds. W.H.G. Lewin and M. van der Klis; astro-ph/0406133 (2004).

4. Borkowski, J., Gotz, D., Mereghetti, S., Mowlavi, N., Shaw, S. *et al.* Giant flare from Sgr 1806-20 detected by INTEGRAL. *GRB Circular Network* **2920**, 1–+ (2004).

5. Boggs, S., Hurley, K., Smith, D. M., Lin, R. P., Hurford, G. *et al.* SGR 1806-20, RHESSI observations of the 041227 giant flare. *GRB Circular Network* **2936**, 1–+ (2005).

6. Cameron, P. B. & Kulkarni, S. R. VLA observations of Sgr 1806-20. *GRB Circular Network* **2928**, 1–+ (2005).

7. Kaplan, D. L., Fox, D. W., Kulkarni, S. R., Gotthelf, E. V., Vasisht, G. *et al.* Precise Chandra Localization of the Soft Gamma-Ray Repeater SGR 1806-20. *ApJ* **564**, 935–940 January 2002.

8. Frail, D. A., Kulkarni, S. R. & Bloom, J. S. An outburst of relativistic particles from the soft gamma-ray repeater SGR 1900+14. *Nature* **398**, 127–129 (1999).

9. Feroci, M., Hurley, K., Duncan, R. C. & Thompson, C. The Giant Flare of 1998 August 27 from SGR 1900+14. I. An Interpretive Study of BeppoSAX and Ulysses Observations. *Astrophys. J.* **549**, 1021–1038 March 2001.

10. Gaensler, B. M., Kouveliotou, C., Wijers, R., Garrett, M., Finger, M. *et al.* Second-epoch VLA observations of Sgr 1806-20. *GRB Circular Network* **2933**, 1–+ (2005).

11. Corbel, S. & Eikenberry, S. S. The connection between W31, SGR 1806-20, and LBV 1806-20: Distance, extinction, and structure. *Astr. Astrophys.* **419**, 191–201 (2004).

12. Kolpak, M. A., Jackson, J. M., Bania, T. M. & Dickey, J. M. The Radial Distribution of Cold Atomic Hydrogen in the Galaxy. *Astrophys. J.* **578**, 868–876 (2002).

13. Corbel, S., Wallyn, P., Dame, T. M., Durouchoux, P., Mahoney, W. A. *et al.* The Distance of the Soft Gamma Repeater SGR 1806-20. *Astrophys. J.* **478**, 624 (1997).

14. Hartmann, D. & Burton, W. B. *Atlas of galactic neutral hydrogen.* Cambridge University Press Cambridge; New York (1997).

15. Garwood, R. W. & Dickey, J. M. Cold atomic gas in the inner Galaxy. *Astrophys. J.* **338**, 841–861 (1989).

16. Figer, D. F., Najarro, F. & Kudritzki, R. P. The Double-lined Spectrum of LBV 1806-20. *Astrophys. J.* **610**, L109–L112 August 2004.

17. Nakar, E., Gal-Yam, A., Piran, T. & Fox, D. B. The distances of short-hard GRBs and the SGR connection. astro-ph/0502148 (2005).

18. Fuchs, Y., Mirabel, F., Chaty, S., Claret, A., Cesarsky, C. J. *et al.* ISO observations of the environment of the soft gamma-ray repeater SGR 1806-20. *Astr. Astrophys.* **350**, 891–899 (1999).

19. Gaensler, B. M., McClure-Griffiths, N. M., Oey, M. S., Haverkorn, M., Dickey, J. M. *et al.* A Stellar Wind Bubble Coincident with the Anomalous X-Ray Pulsar 1E 1048.1-5937: Are Magnetars Formed from Massive Progenitors? *Astrophys. J.* **620**, L95–L98 February 2005.

20. Pacholczyk, A. G. *Radio astrophysics. Nonthermal processes in galactic and extragalactic sources.* Series of Books in Astronomy and Astrophysics, San Francisco: Freeman, 1970 (1970).

21. Scott, M. A. & Readhead, A. C. S. The low-frequency structure of powerful radio sources and limits to departures from equipartition. *Mon. Not. R. astr. Soc.* **180**, 539–550 September 1977.

22. Frail, D. A., Waxman, E. & Kulkarni, S. R. A 450 Day Light Curve of the Radio Afterglow of GRB 970508: Fireball Calorimetry. *Astrophys. J.* **537**, 191–204 (2000).

23. Cheng, K. S. & Wang, X. Y. The Radio Afterglow from the Giant Flare of SGR 1900+14: The Same Mechanism as Afterglows from Classic Gamma-Ray Bursts? *Astrophys. J.* **593**, L85–L88 (2003).

24. Nakar, E., Piran, T. & Sari, R. Giant flares as mini gamma ray bursts. astro-ph/0502052 (2005).

25. Wang, X. Y., Wu, X. F., Fan, Y. Z., Dai, Z. G. & Zhang, B. An energetic blast wave from the december 27 giant flare of soft γ-ray repeater 1806−20. astro-ph/0502085 (2005).

26. Hjellming, R. M., Rupen, M. P., Hunstead, R. W., Campbell-Wilson, D., Mioduszewski, A. J. *et al.* Light Curves and Radio Structure of the 1999 September Transient Event in V4641 Sagittarii (=XTE J1819-254=SAX J1819.3-2525). *Astrophys. J.* **544**, 977–992 (2000).

Supplementary Information accompanies the paper on **www.nature.com/nature.**

Acknowledgements

Correspondence and requests for materials should be addressed to P.B.C. (pbc@astro.caltech.edu).

FIGURES & CAPTIONS

Table 1: Flux density measurements of the transient radio counterpart to SGR 1806−20 from the VLA, GMRT, NMA, and ATCA as a function of frequency and time. The reported errors are 1-σ. In addition to these measurements, we obtained IRAM-30m observations on 8 and 9 January 2005 using MAMBO-2 at 250 GHz which show no detection with a value of 0.57 ± 0.46 mJy at the position of the radio source. Finally, we detect linearly polarized emission from the source at the 1.5% to 2.5% level. See the Supplemental Information for observational details.

[a] The epoch of the flare, t_0, was 27.90 December 2004.

[b] ATCA observations in this column have a frequency of 8.6 GHz.

[c] These values represent 2σ upper limits.

[d] The frequency is 1.06 GHz for the 16.37 January 2005 and 4.01 February 2005 GMRT observations.

Figure 1: Broadband temporal behavior of the transient radio source coincident with SGR 1806−20. The abscissa indicates days elapsed since the giant flare on 27.90 December 2004. The displayed flux density measurements (denoted with symbols) were obtained in six frequency bands with the VLA, GMRT, and ATCA (Table 1). The error bars denote 1-σ uncertainties. With the exception of the 6.1 GHz data (which is insufficiently sampled at early and late times and is not shown), the light curves with $\nu > 1$ GHz are best fit by power-law models (shown as lines, $S_\nu \propto t^{\alpha_i}$) with two breaks at $t_1 \sim 9$ days and $t_2 \sim 15$ days (see the Supplemental Information for exact values). The temporal index varies chromatically in the time before and after the first break (denoted by regions A and B respectively). The exponent value ranges from $-2 \lesssim \alpha_A \lesssim -1$ and $-4 \lesssim \alpha_B \lesssim -3$; here the subscript identifies the region of interest. After day ~ 15 (region C) the source decay flattens to $\alpha_C \sim -0.9$ at these frequencies which persists until day 51. Region B, the period of steep light curve decline, is shaded gray. The light curves with $\nu < 1$ GHz do not show these temporal breaks or late time flattening Apparently a single power law decay model with $\alpha = -1.57 \pm 0.11$ (0.24 GHz) and $\alpha = -1.80 \pm 0.08$ (0.61 GHz) provides a good statistical description of the data.

Our substantial frequency coverage (over three decades) allows an excellent characterization of the spectrum. The spectrum is consistent with a single power law slope ($S_\nu \propto \nu^\beta$) at all epochs. On day 7, before the first temporal break, we find $\beta = -0.62 \pm 0.02$. The spectrum

steepens to a value of $\beta = -0.76 \pm 0.05$ (day 15), reaching $\beta = -0.9 \pm 0.1$ (days 21–51).

Table 2: Source size measurements and 95% confidence limits of the radio source as measured with the VLA at 8.46 GHz. The source is clearly resolved at all VLA epochs. The best constraints on the source size come from the observations which occurred closest to the transit of the source on Jan 3rd and Jan 6th. The result is a source with size $\theta \sim 77$ mas with an axial ratio of ~ 0.5 and a position angle (PA) of 60 degrees (measured clockwise from the North). The flux centroid did not change position within the limits of our astrometric accuracy ($\pm$ 100 mas).

The best fit model is consistent with no expansion, $s = 0.04 \pm 0.15$ ($\theta(t) \propto t^s$) with a $\chi^2 = 5.3$ with 4 degrees of freedom. Sedov-Taylor ($s = 2/5$) and free expansion ($s = 1$) model were also fit, and yield $\chi^2 = 20.6$ and $\chi^2 = 91$, respectively. These fits have five degrees of freedom. See the Supplemental Information for the details of the source size measurements.

Figure 2: Cold atomic and molecular hydrogen spectra toward SGR 1806−20. These spectra were used to derive a distance estimate for SGR 1806−20. *(Top Panel).* HI emission (upper curve, thick line) in the direction of SGR 1806−20, determined by averaging two adjacent spectra taken by Hartmann & Burton[14] at l,b=(10.0°,0.0°) and l,b=(10.0°,−0.5°). The lower curve (thin line) is the ^{12}CO(1−0) spectrum (from ref. 11). For display purposes the brightness temperature has been scaled up by a factor of 11.4. *(Second Panel).* The HI absorption spectrum taken toward SGR 1806−20. The two horizontal bars illustrate the radial velocity measurements[16,11] of the nearby star LBV 1806−20 ($36 \pm 10\ \mathrm{km\,s^{-1}}$ and $10 \pm 20\ \mathrm{km\,s^{-1}}$). The absorption spectra were made with the Very Large Array on 4 January 2005, using a 1.56 MHz bandwidth in both hands of polarization centered $50\ \mathrm{km\,s^{-1}}$ with respect to the local standard of rest. The bandwidth was divided into 256 channels each 6.1 kHz in width, or a velocity resolution of 1.3 $\mathrm{km\,s^{-1}}$ covering a velocity range of $-115\ \mathrm{km\,s^{-1}}$ to $+215\ \mathrm{km\,s^{-1}}$. *(Third Panel).* The distance as a function of radial velocity adopting a simple Galactic rotation curve with a circular velocity $\Theta_\circ = 220\ \mathrm{km\,s^{-1}}$ and a galactic center distance R$_\circ$=8.5 kpc. *(Bottom Panel).* The HI absorption spectrum of nearby extragalactic source J1811−2055 at l,b=(9.8°,−1.0°).

The lower limit to the distance is firmly established by the $95\ \mathrm{km\,s^{-1}}$ absorption feature from MC94 (see Text). An upper limit to the distance of the SGR is suggested by the *absence* of strong absorption at $+120\ \mathrm{km\ s^{-1}}$, seen toward J1811−2055 and several other extragalactic radio sources in this direction.[15] One could argue that the $120\ \mathrm{km\,s^{-1}}$ cold cloud is small and

not present along the line-of-sight to the SGR 1806−20. However, this hypothesis also requires the absence of any other cloud between $95 \, \mathrm{km \, s^{-1}}$ (distance of 6.4 kpc) and $86 \, \mathrm{km \, s^{-1}}$ (distance of 10.6 kpc). The mean absorption coefficient drops in the inner Galaxy ($R \lesssim 4.5$) kpc, giving a mean free path between clouds of 2.3 kpc.[15] The distance interval from 6.4 kpc to 10.6 kpc corresponds to ~ 1.8 mean free paths. So, the probability of finding no clouds in this gap is 16%. Thus our upper limit of 9.8 kpc is not a certainty but quite likely.

Epoch	Telescope	Δt^a (days)	$S_{0.24}$ (mJy)	$S_{0.610}$ (mJy)	$S_{1.46}$ (mJy)	$S_{2.4}$ (mJy)	$S_{4.86}$ (mJy)	$S_{6.1}$ (mJy)	$S_{8.46}^b$ (mJy)	S_{102} (mJy)
3.84 Jan 2005	VLA	6.94	—	—	178 ± 4	—	79 ± 2	—	53 ± 1	—
4.17 Jan 2005	NMA	7.27	—	—	—	—	—	—	—	16.3 ± 5.6
4.41 Jan 2005	GMRT	7.51	466 ± 28	224 ± 13	—	—	—	—	—	—
4.59 Jan 2005	VLA	7.69	—	—	161 ± 4	—	66 ± 2	—	44 ± 1	—
5.26 Jan 2005	ATCA	8.36	—	—	127 ± 3	80 ± 2	—	—	—	—
5.66 Jan 2005	VLA	8.76	—	—	—	—	55 ± 1	—	33 ± 1	—
5.85 Jan 2005	ATCA	8.93	—	—	113 ± 3	63 ± 2	53 ± 2	—	30 ± 1	—
6.26 Jan 2005	ATCA	9.36	—	—	96 ± 3	73 ± 2	45 ± 2	—	23 ± 1	—
6.38 Jan 2005	GMRT	9.48	462 ± 29	142 ± 8	—	—	—	—	—	—
6.77 Jan 2005	VLA	9.87	—	—	93 ± 2	—	38 ± 1	—	23.5 ± 0.5	—
6.77 Jan 2005	ATCA	9.87	—	—	85 ± 3	67 ± 2	40 ± 1	32 ± 1	—	—
7.20 Jan 2005	ATCA	10.30	—	—	88 ± 2	55 ± 1	—	—	—	—
7.25 Jan 2005	GMRT	10.35	231 ± 20	125 ± 9	—	—	—	—	—	—
7.90 Jan 2005	VLA	11.00	—	—	71 ± 2	—	26 ± 1	—	16.5 ± 0.5	—
8.19 Jan 2005	ATCA	11.29	—	—	67 ± 3	38 ± 2	24 ± 1	20 ± 1	—	—
8.24 Jan 2005	GMRT	11.34	250 ± 17	104 ± 8	—	—	—	—	—	—
9.06 Jan 2005	ATCA	12.16	—	—	42 ± 2	32 ± 1.5	21 ± 1	—	11.4 ± 1	—
9.26 Jan 2005	GMRT	12.36	176 ± 20	86 ± 7	—	—	—	—	—	—
10.07 Jan 2005	ATCA	13.16	—	—	32 ± 2	24 ± 1	17 ± 1	—	10 ± 1	—
10.16 Jan 2005	GMRT	13.26	155 ± 17	82 ± 7	—	—	—	—	—	—
10.60 Jan 2005	VLA	13.70	—	—	—	—	—	—	8.7 ± 0.4	—
12.00 Jan 2005	NMA	15.10	—	—	—	—	—	—	—	7.16^c
12.04 Jan 2005	ATCA	15.14	—	—	24 ± 1.5	16 ± 1	12 ± 1	9.3 ± 1	7.3 ± 1	—
13.00 Jan 2005	NMA	16.10	—	—	—	—	—	—	—	5.50^c
14.04 Jan 2005	ATCA	17.14	—	—	23 ± 1	15 ± 1	9.7 ± 1	7.3 ± 1	5.5 ± 1	—
16.25 Jan 2005	GMRT	19.35	96 ± 23	31 ± 5	—	—	—	—	—	—
16.37 Jan 2005	GMRT	19.47	—	—	$20 ± 2^d$	—	—	—	—	—
18.01 Jan 2005	ATCA	21.11	—	—	24 ± 1.5	17 ± 1	6.2 ± 1	4.7 ± 1	3.8± 1	—
20.10 Jan 2005	ATCA	23.20	—	—	19 ± 1.5	10 ± 1.5	5 ± 1	—	3.2± 1	—
22.07 Jan 2005	ATCA	25.17	—	—	18 ± 1	11 ± 1	5 ± 1	4.3± 1	2.0± 1	—
23.84 Jan 2005	ATCA	26.94	—	—	12 ± 1	7.9 ± 1	5.6 ± 1	3.7± 1	3.6± 1	—
24.85 Jan 2005	ATCA	27.95	—	—	12 ± 1	11 ± 1	4.2 ± 1	5.1± 1	3.6± 1	—
26.26 Jan 2005	GMRT	29.36	104 ± 31	19 ± 6	—	—	—	—	—	—
4.01 Feb 2005	GMRT	38.14	—	—	$10^{c,d}$	—	—	—	—	—
16.87 Feb 2005	ATCA	50.97	—	—	10 ± 1	6.3 ± 1	3.3 ± 0.4	—	2.1 ± 0.3	—
24.01 Feb 2005	GMRT	58.11	28.2 ± 9	6.6 ± 1.4	—	—	—	—	—	—

Table 1.

Epoch	Beam (mas)	Beam PA (degrees)	Fit Major Axis (mas)	Axial Ratio	Fit PA (degrees)
03 Jan 2005	349×170	11.8	$78.2^{+3.0}_{-2.9}$	$0.34^{+0.21}_{-0.34}$	$54.6^{+6.7}_{-6.0}$
04 Jan 2005	593×173	-40.3	$72.4^{+14.5}_{-48}$	$0.00^{+0.90}_{-0}$	69^{+20}_{-67}
05 Jan 2005	397×168	-25.7	55^{+18}_{-10}	$0.66^{+0.34}_{-0.66}$	74^{+90}_{-90}
06 Jan 2005	329×178	-16.5	$75.7^{+3.0}_{-3.0}$	$0.48^{+0.18}_{-0.33}$	$51.8^{+9.0}_{-8.8}$
07 Jan 2005	532×178	40.4	78^{+26}_{-18}	$0.60^{+0.4}_{-0.60}$	69^{+90}_{-90}
10 Jan 2005	560×161	-38.8	112^{+30}_{-42}	$0.34^{+0.33}_{-0.34}$	18^{+28}_{-18}

Table 2.

Figure 1.

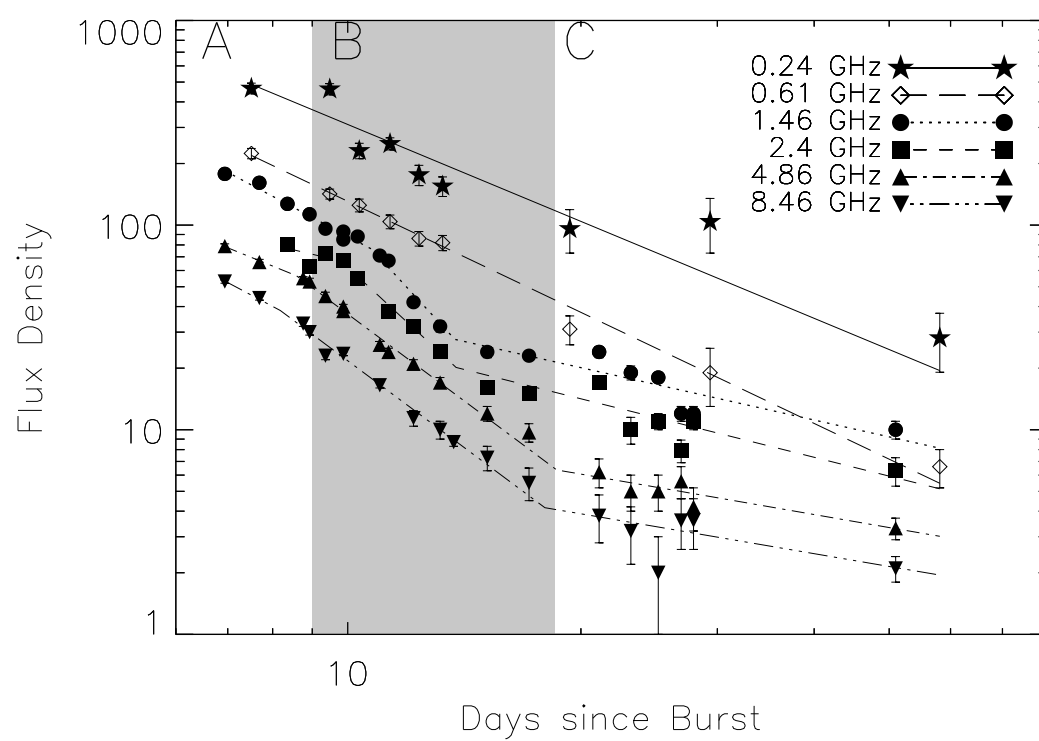
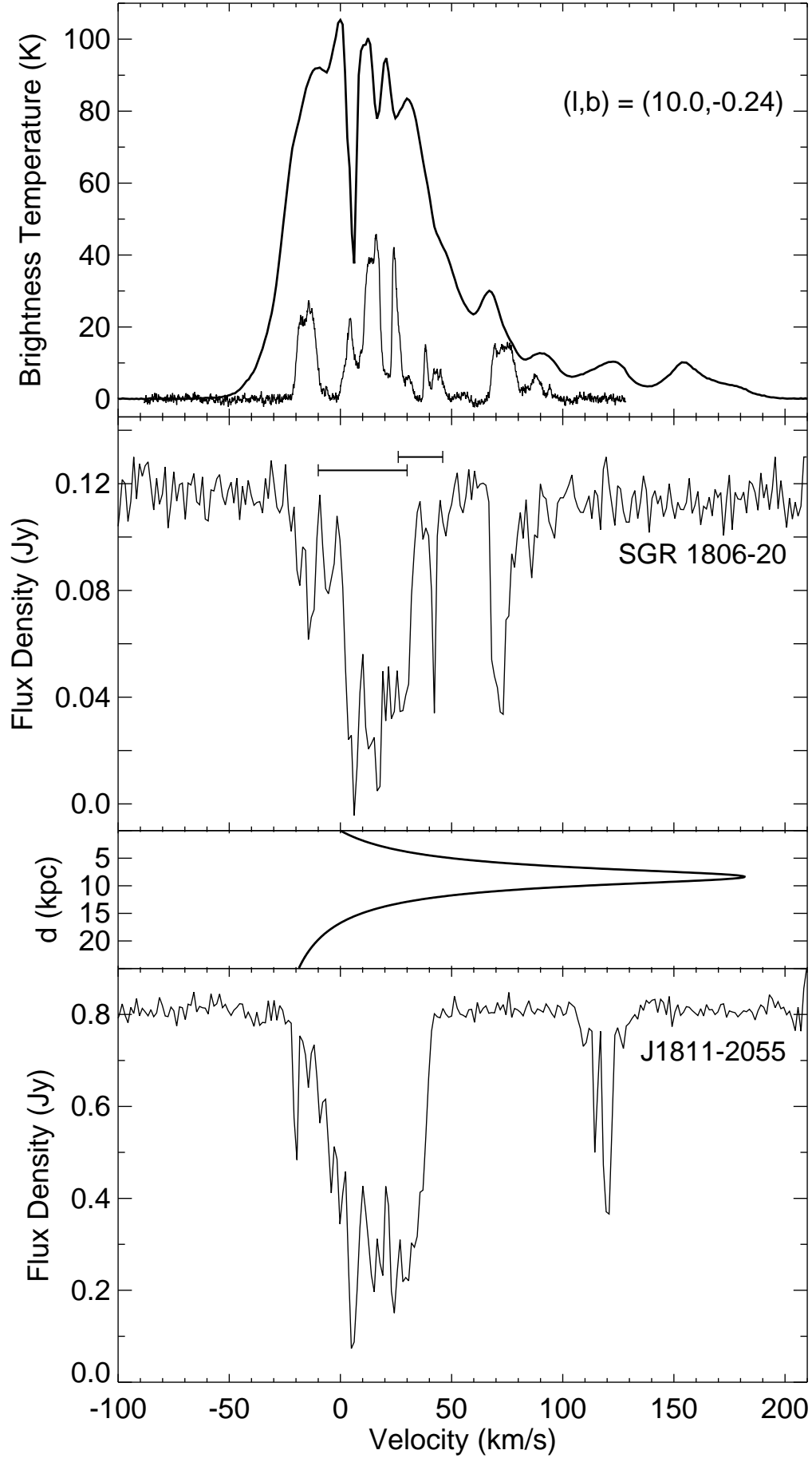
Figure 2.

SUPPLEMENTAL INFORMATION

Observational Details: For the VLA observations we used the standard continuum mode with 2×50 MHz bands, with the exception of the 1.46 GHz observation of 4 January 2005, which was taken in spectral line mode with 8 channels of width 3.1 MHz. We used the extragalactic source 3C 286 (J1331+305) for flux calibration, while the phase was monitored with J1820-254, J1751−253, and J1811−209. The listed flux densities and uncertainties were measured from the resulting maps by fitting an elliptical Gaussian model to the afterglow emission. The GMRT observations were performed in dual frequency mode with 16 MHz bandwidth divided into a total of 128 frequency channels for 610 MHz observations, and 6 MHz of bandwidth divided into 64 channels for the 235 MHz observations. The observations at 1060 MHz at GMRT were carried out with a bandwidth of 32 MHz. 3C 48 (J0137+331) and 3C 286 were used as flux calibrators, and J1822−096 was used as the phase calibrator. These sources were also used for bandpass calibration. We obtained the flux densities of the source by fitting a Gaussian with a background level plus a slope and removed the contribution from a nearby weak source. Because of the high density of radio sources in the galactic plane in which SGR 1806−20 is located, the antenna system noise temperature has notable contributions from the sky within the telescope beam. This reduces the signal to noise ratio and an appropriate correction must be made to the observed flux (especially at low frequencies), since the flux calibrators which establish the flux scale lie well outside the galactic plane and are in an environment of less sky temperature. We applied a T_{sys} correction factor for 3C 48 of 3.88 and 1.93, and for 3C 286 of 3.87 and 1.8, for the 235 MHz and 610 MHz, respectively. Both the VLA and GMRT data were reduced and analyzed using the Astronomical Image Processing System. The ATCA observations were performed in snapshot mode with 100MHz of effective bandwidth. The amplitude calibrator was J1934−638, whereas J1711−251, J1817−254, and J1811−209 where used as phase calibrators. The last of these was observed in a rapid (3 minute) cycle mode to compensate for its poor phase stability. The flux densities were determined by performing a local parabolic fit to the peak closest to the known position of the source. The NMA observations were performed at 102 GHz in D-configuration (the most compact configuration) on 4 January 2005, and in AB configuration (longest baseline configuration) on 12, 13 January 2005. We used NRAO530 for

the phase calibration, and assumed it to have a flux density of 2.3 Jy.

Details of Source Size Measurements: The source sizes were measured by modeling the calibrated visibilities with the model-fitting procedure in DIFMAP. This procedure employs the Levenberg-Marquardt non-linear least squares minimization technique while fitting a 6 parameter elliptical Gaussian to the visibilities. The errors were determined with DIFWRAP using the following scheme: the source size parameters were stepped in small increments around their best-fitted value to form a grid of values. At each grid point the source size parameters were held fixed while the other model parameters were allowed to 'relax' with 4 model-fitting rounds. The 95% confidence limits were determined by those models that had a $\Delta\chi^2 < 12.8$ as measured from the best-fit total χ^2 (Press, W. H., Teukolsky, S. A., Vetterling, W. T. and Flannery, B. P. *Numerical Recipies in C. The art of scientific computing.* Cambridge: University Press, 2nd ed. 1992). As a check we used phase only self-calibration as well as phase and amplitude self-calibration, both of which give consistent source size measurements. We also used 30 second time-averaged data sets (to reduce the number of degrees of freedom), and found the best fit model parameters agreed to within the errors.

Frequency (GHz)	α_A	t_1 (days)	α_B	t_2 (days)	α_C
0.240	-1.7 ± 0.1	—	—	—	—
0.61	-1.9 ± 0.1	—	—	—	—
1.4	-2.0 ± 0.2	10.7 ± 0.3	-4.1 ± 0.3	13.8 ± 0.2	-0.85 ± 0.2
2.4	-0.95 ± 0.3	9.8 ± 0.2	-3.5 ± 0.2	13.8 ± 0.5	-0.95 ± 0.2
4.9	-1.55 ± 0.15	8.8 ± 0.2	-3.1 ± 0.2	18.6 ± 3.0	-0.65 ± 0.3
6.1	-2.3 ± 0.1	—	—	—	—
8.5	-2.00 ± 0.15	8.1 ± 0.3	-2.8 ± 0.24	18.0 ± 3.0	-0.64 ± 0.4

Table : Summary of temporal indices and breaks in the light curve of SGR 1806−20 in 7 frequency bands. The fits represent minimums in χ^2 subject to the conditions that the two power-law slopes are continuous at the break point and disagree by more than 1-σ. The first and second break points are denoted by t_1 and t_2, respectively. The temporal decay indices ($S_\nu \propto t^{\alpha_i}$) are α_A for $t < t_1$, α_B for $t_1 < t < t_2$, and α_C for $t > t_2$.